JBC RESEARCH ARTICLE

The RNA helicase DHX36–G4R1 modulates C9orf72 GGGGCC hexanucleotide repeat–associated translation

Received for publication, April 27, 2021, and in revised form, June 2, 2021 Published, Papers in Press, June 24, 2021,
https://doi.org/10.1016/j.jbc.2021.100914

Yi-Ju Tseng[1,2], Siara N. Sandwith[3], Katelyn M. Green[1], Antonio E. Chambers[3], Amy Krans[1], Heather M. Raimer[4], Meredith E. Sharlow[3], Michael A. Reisinger[3], Adam E. Richardson[3], Eric D. Routh[5], Melissa A. Smaldino[3], Yuh-Hwa Wang[4], James P. Vaughn[6], Peter K. Todd[1,7,*], and Philip J. Smaldino[3,*]

From the [1]Department of Neurology, [2]Cellular and Molecular Biology Graduate Program, University of Michigan, Ann Arbor, Michigan, USA; [3]Department of Biology, Ball State University, Muncie, Indiana, USA; [4]Department of Biochemistry and Molecular Genetics, University of Virginia, Charlottesville, Virginia, USA; [5]Lineberger Comprehensive Cancer Center, University of North Carolina at Chapel Hill, Chapel Hill, North Carolina, USA; [6]Division of Cancer Biology, NanoMedica LLC, Winston-Salem, North Carolina, USA; [7]Department of Neurology, Ann Arbor VA Medical Center, Ann Arbor, Michigan, USA

Edited by Ronald Wek

GGGGCC (G_4C_2) hexanucleotide repeat expansions in the endosomal trafficking gene *C9orf72* are the most common genetic cause of ALS and frontotemporal dementia. Repeat-associated non-AUG (RAN) translation of this expansion through near-cognate initiation codon usage and internal ribosomal entry generates toxic proteins that accumulate in patients' brains and contribute to disease pathogenesis. The helicase protein DEAH-box helicase 36 (DHX36–G4R1) plays active roles in RNA and DNA G-quadruplex (G4) resolution in cells. As G_4C_2 repeats are known to form G4 structures *in vitro*, we sought to determine the impact of manipulating DHX36 expression on repeat transcription and RAN translation. Using a series of luciferase reporter assays both in cells and *in vitro*, we found that DHX36 depletion suppresses RAN translation in a repeat length–dependent manner, whereas overexpression of DHX36 enhances RAN translation from G_4C_2 reporter RNAs. Moreover, upregulation of RAN translation that is typically triggered by integrated stress response activation is prevented by loss of DHX36. These results suggest that DHX36 is active in regulating G_4C_2 repeat translation, providing potential implications for therapeutic development in nucleotide repeat expansion disorders.

A GGGGCC (G_4C_2) hexanucleotide repeat expansion (HRE) within the first intron of *C9orf72* is a major genetic cause of ALS and frontal temporal dementia (C9 FTD/ALS) (1, 2). Typically, humans have ~2 to 28 repeats, whereas disease-associated alleles have >30 and often hundred to thousand repeats (3, 4). C9 FTD/ALS represents over 40% of the familial cases and upward of 10% of the sporadic cases of ALS in European populations (5). Despite intense research efforts since its discovery in 2011, C9 FTD/ALS remains a progressive and fatal condition without effective treatment (1, 2, 6).

Both DNA and RNA G_4C_2 HRE sequences are prone to folding into G-quadruplex (G4) structures *in vitro* (6–13). G4 structures are dynamic and nucleic acid secondary structures consisting of an assembly of vertically stacked guanine-tetrad building blocks. G4 structures are stabilized by Hoogsteen hydrogen bonding and monovalent cations, especially K^+ (14–16). G4 structures have been directly observed in human cells (17–19), with >700,000 G4 motifs residing throughout the human genome (20, 21). G4 structure motifs are non-randomly distributed, with enrichment in gene promoters, UTRs, and origins of replication, suggesting functional roles in transcription, translation, and replication, respectively (20–24). Taken together, G4 structures are linked to each of the major toxicities observed in C9 FTD/ALS patient neurons.

The underlying pathogenesis of the G_4C_2 HRE involves at least three inter-related pathways, each of which is foundationally linked to aberrant G4 structures. The G_4C_2 HRE as DNA impairs mRNA transcription and alters the epigenetics of the *C9orf72* locus, decreasing C9orf72 protein expression (25). Endogenous C9orf72 protein is important for endosomal trafficking and autophagy in neurons, and its loss is detrimental to neurons and impacts inflammatory pathways relevant to ALS (25). When transcribed, the resultant G_4C_2 mRNA species folds into G4 structures, which coalesce as RNA foci in complex with RNA-binding proteins, impairing RNA processing (2, 6). If transcribed G_4C_2 HRE mRNAs reach the cytoplasm, they can serve as a template for repeat-associated non-AUG–initiated (RAN) translation. RAN translation from G_4C_2-repeat RNA (C9RAN) produces dipeptide repeat proteins (DPRs) that aggregate in proteinaceous inclusions. C9RAN DPRs cause proteotoxic stress and disrupt nucleocytoplasmic transport (13, 26, 27).

The mechanisms underlying C9RAN remains enigmatic (28). Initiation can occur at either an upstream near-AUG codon (CUG) or within the repeat itself (29–32). RNA helicases such as eukaryotic translation initiation factor 4B, eukaryotic translation initiation factor 4H, and DDX3X play active and selective roles in the translation process, as do the ribosomal accessory protein, ribosomal protein S25 (33–36). RAN translation also demonstrates a selective enhancement in

* For correspondence: Philip J. Smaldino, pjsmaldino@bsu.edu; Peter K. Todd, petertod@med.umich.edu.

response to cellular stress pathways, which activate stress granule (SG) formation and suppress global translation through phosphorylation of eukaryotic translation initiation factor 2 subunit alpha (29–31, 37, 38). Consistent with this, modulation of the alternative ternary complex protein eukaryotic translation initiation factor 2A or protein kinase R expression can alter C9RAN translation (32, 38).

Given their potentially central role in G_4C_2 repeats in C9 FTD/ALS pathogenesis, we explored factors responsible for G4 resolution within cells. One such enzyme, DHX36 (aliases: G4R1 and RHAU), is a member of the DExH-box family of helicases (39). DHX36 accounts for the majority of the tetramolecular G4 DNA and RNA helicase activity in HeLa cell lysates (40, 41). DHX36 binds to a diverse array of unimolecular DNA and RNA G4 structures with the tightest affinity of any known G4 structure–binding protein and can catalytically unwind these structures in isolation (6, 42–52). DHX36 associates with thousands of G4-containing DNA and mRNA sequences, facilitating both their transcription and translation (53–55). Moreover, DHX36 plays an active role in SG dynamics, where its loss can trigger spontaneous formation of SGs and changes in their dissolution after a transient stress exposure (53). Thus, DHX36 has the potential to influence *C9orf72* transcription and G_4C_2-repeat RNA stability, localization, and RAN translation (23, 44).

Here, we find that DHX36 knockdown (KD) and KO selectively suppresses C9RAN translation as well as RAN translation at CGG repeats from reporters in human cells. In contrast, overexpression of WT DHX36, but not a mutant form of DHX36 that lacks helicase activity, enhances RAN translation. These effects are largely translational as we observe suppression of C9RAN translation in an *in vitro* DHX36 KO cell lysate translation system while observing no significant alterations in reporter RNA in response to KD or overexpression of DHX36. Loss of DHX36 also precludes stress-dependent upregulation of C9RAN translation consistent with its role in SG formation. Taken together, these results suggest modulation of G4 structures at the RNA level by candidate G4 helicases such as DHX36 impact G_4C_2-repeat expansion translation implicated in C9 FTD/ALS.

Results

DHX36 directly binds C9-repeat G4 DNA in vitro

To determine if DHX36 directly binds to C9 G4 DNA structures, we performed EMSAs with a DNA oligonucleotide composed of five G_4C_2 repeats with a 3′ unstructured tail shown to be required for G4 binding (47, 56) (referred to hereafter as "$(G_4C_2)_5$-DNA"). $(G_4C_2)_5$-DNA was folded into G4 structures by heating and cooling in the presence of potassium chloride (KCl). As a negative control non-G4 DNA, $(G_4C_2)_5$-DNA was heated and cooled in the absence of KCl. G4 $(G_4C_2)_5$-DNA and non-G4 $(G_4C_2)_5$-DNA were incubated with purified recombinant DHX36 (rDHX36) under noncatalytic conditions (−ATP, +EDTA) so that binding could be visualized on a gel (Fig. 1, *A* and *C*). As an additional control, this was repeated with scrambled C9-repeat DNA, where the C9-repeat sequence was rearranged as to prevent G4 structure formation (Fig. 1, *B* and *C*). Following incubation, the samples were subjected to nondenaturing PAGE. In the absence of KCl, a single band is observed for $(G_4C_2)_5$-DNA. When KCl is added, slower migrating bands are observed, consistent with the formation of G4 structures. Incubation of $(G_4C_2)_5$-DNA with rDHX36 resulted in a shift of the DNA to the upper region of the gel indicating direct binding. Notably, some unstructured $(G_4C_2)_5$-DNA is present in the KCl-containing reactions and is not bound by DHX36, further suggesting selective binding to G4 structure. In the absence of KCl (*i.e.*, non-G4 conditions), binding of rDHX36 to $(G_4C_2)_5$-DNA is substantially reduced. Furthermore, scrambled $(G_4C_2)_5$-DNA does not form KCl-dependent higher-ordered structures and is not a strong binding substrate for rDHX36 even in the presence of KCl. Taken together, these data suggest that DHX36 directly binds to C9 HRE DNA in a G4-dependent manner *in vitro*.

DHX36 enhances transcription of C9-repeat DNA in vitro

G4 DNA structures impede the transcription of C9-repeat RNA and T7 elongation (6). Given that DHX36 is a helicase that resolves G4 structures, we hypothesized that DHX36 might facilitate the transcription of C9-repeat RNA. To test this, we performed an *in vitro* transcription assay with a plasmid containing 70 G_4C_2 repeats (pCR8-$(G_4C_2)_{70}$) driven by a T7 RNA polymerase reporter (27). We incubated the plasmid with T7 polymerase in the presence and absence of rDHX36. A T7 plasmid containing a nanoluciferase (NLuc) gene was used as a non-G4 control. The resulting RNA transcripts were subjected to denaturing urea gel electrophoresis. We found that rDHX36 significantly increased the length of RNA transcripts yielded from G_4C_2-repeat DNA but not from NLuc (Fig. 1, *D* and *E*). However, the total RNA generated from G_4C_2-repeat DNA and NLuc DNA was not significantly different between rDHX36 and control (Ctrl) reactions (Fig. S1). These data suggest that rDHX36 facilitates efficient and complete *in vitro* transcription of G4 C9-repeat sequences by T7 RNA polymerase but may not impact its overall production.

DHX36 depletion modifies C9RAN translation

We next evaluated the impact of altering DHX36 expression on C9RAN translation. To accomplish this, we utilized previously described C9RAN translation–specific NLuc reporters (C9-NLuc) (29). These reporters include 70 G_4C_2 repeats in the context of the first *C9orf72* intron. This sequence is inserted 5′ to an NLuc whose start codon is mutated to GGG and with a 3× FLAG tag fused to its carboxyl terminus (Fig. 2*A*). Single base-pair insertions between the repeat and NLuc allow for evaluation of translation in all three reading frames. An AUG-initiated NLuc serves as a positive control for canonical translation. An AUG-initiated firefly luciferase (FFLuc) is included as a transfection control (29).

To study the effects of loss of DHX36, we used a previously described stable and inducible KD (DHX36 KD) HeLa cell line (41, 57) (Fig. 2*B* and Fig. S2, *A*–*E*). Treatment of these cells

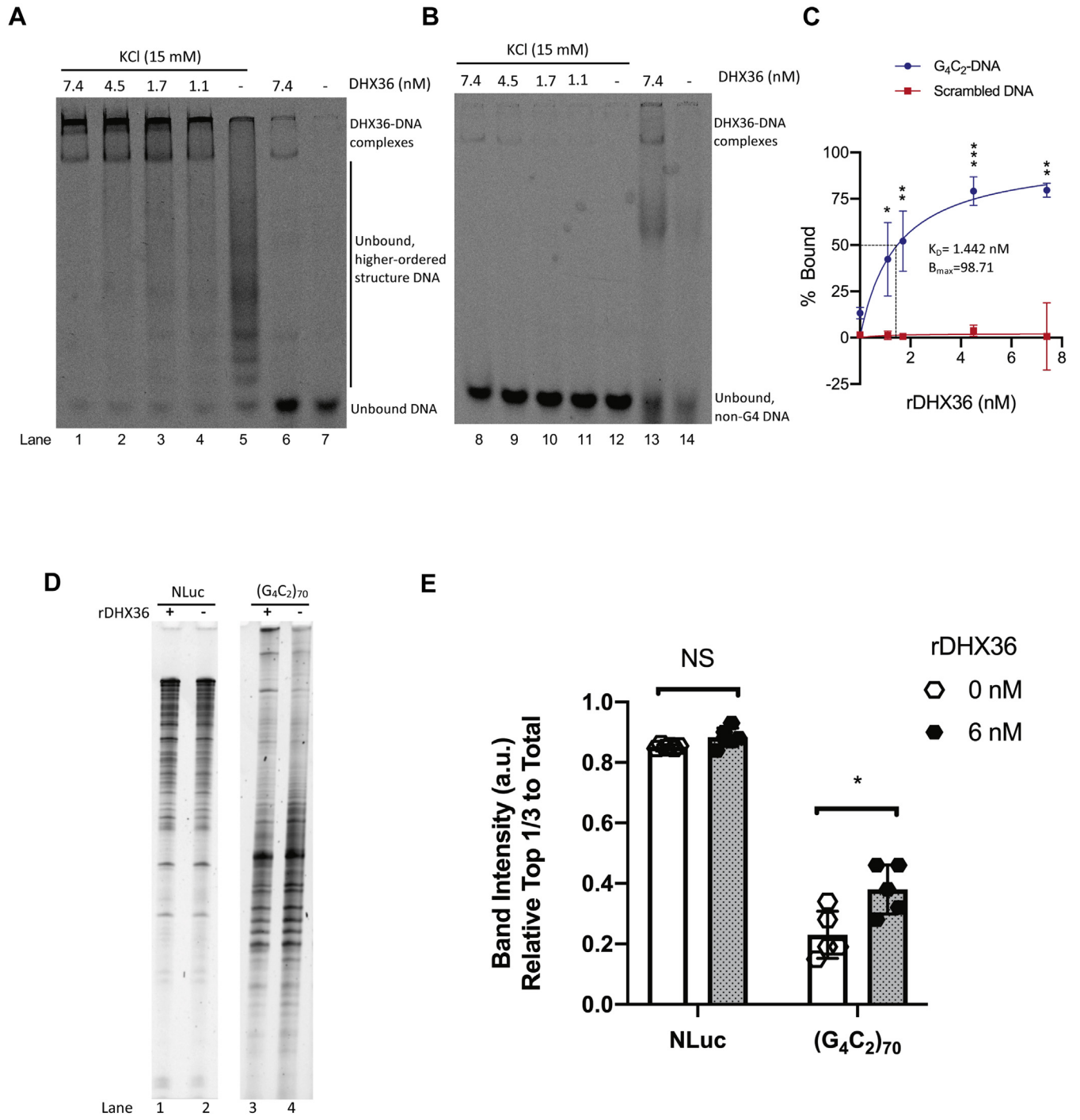

Figure 1. DHX36 binds and enhances transcription of C9-DNA *in vitro*. *A*, representative EMSA image. C9-repeat DNA oligonucleotides were heated and cooled in the presence (lanes 1–5) and absence (lanes 6 and 7) of KCl to induce or prevent G4 formation, respectively. DNA was incubated with increasing concentrations of recombinant DHX36, analyzed with nondenaturing PAGE, and imaged. *B*, representative EMSA image. Scrambled control DNA oligonucleotides were heated and cooled in the presence (lanes 1–5) and absence (lanes 6 and 7) of KCl. DNA was incubated with increasing concentrations of recombinant DHX36, analyzed with nondenaturing PAGE, and imaged. *C*, densiometric quantification of panels *A* and *B*. The percent bound for each lane was graphed *versus* the concentration of DHX36. Data are presented as mean ± SD, n = 3. Multiple *t* tests for each concentration of protein, $*p \le 0.05$, $**p < 0.01$, and $***p < 0.001$. *D*, T7 polymerase transcript products generated from equal amounts of linearized NLuc (lanes 1 and 2) or $(G_4C_2)_{70}$ plasmids (lanes 3 and 4) resolved by denaturing PAGE. The gel was stained with SYBR gold nucleic acid stain and imaged. *E*, densiometric quantification of panel *D*. All signals were first subtracted by the background. Then signal from the top third of the gel was divided by the total signal per lane. Data are presented as mean ± SD, n = 5 for (NLuc)-6$(G_4C_2)_{70}$. Two-tailed paired *t* test, $*p < 0.05$. DHX36, DEAH-box helicase 36; KCl, potassium chloride; NLuc, nanoluciferase; NS, not significant.

with doxycycline (doxy) for 96 h significantly reduced DHX36 expression as measured by immunoblot (Fig. 2*C*). Comparing between Ctrl and DHX36 KD cells with transiently transfected C9-NLuc reporters, DHX36 KD selectively decreased C9RAN translation in the GA (+0), GP (+1), and GR (+2) reading frames, relative to AUG-NLuc when normalized to

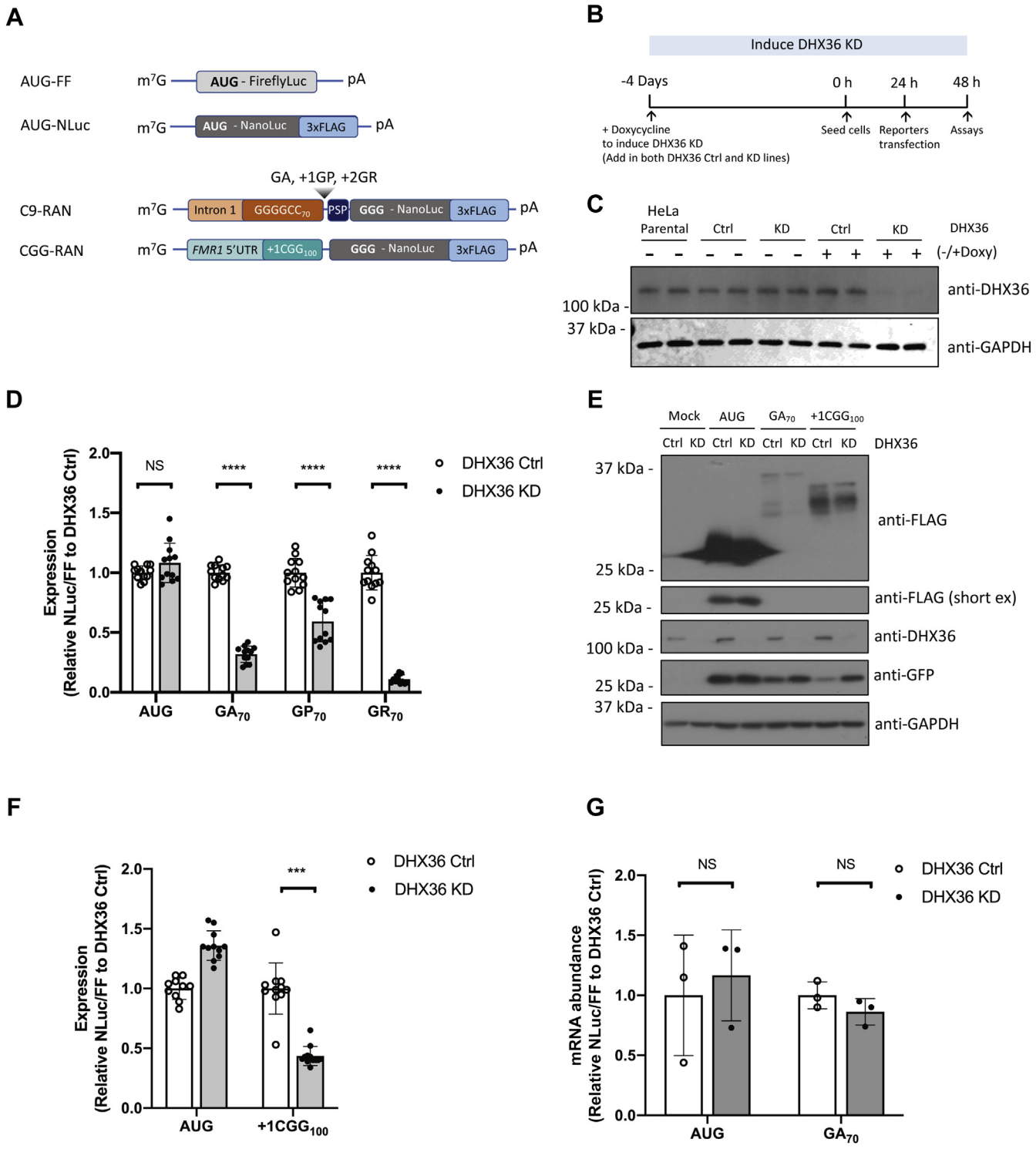

Figure 2. The effect of DHX36 KD on C9-RNA and C9RAN reporter expression. *A*, schematic of AUG-FF, AUG-NLuc Ctrl, C9-RAN, and CGG-RAN luciferase reporters. *B*, experimental timeline for doxycycline treatment and reporter transfection. *C*, immunoblots detecting DHX36 in parental, Ctrl, and DHX36 KD HeLa cells with and without doxycycline treatment. *D*, relative expression of AUG and C9-RAN translation in GA (+0), GP (+1), and GR (+2) frames with 70 repeats between Ctrl and DHX36 KD HeLa cells. NLuc signals were normalized to AUG-FFluc translation. *E*, immunoblot of RAN translation products from 70 repeats of G_4C_2 in GA frame and 100 repeats of CGG in +1 reading frame in Ctrl and DHX36 KD HeLa cells. GFP was blotted as transfection control, and GAPDH was blotted as loading Ctrl. *F*, expression of $+1CGG_{100}$ RAN translation reporters measured by luciferase assay. NLuc signals were normalized to AUG-FFluc signals to compare between Ctrl and DHX36 KD HeLa cells. *G*, abundance of NLuc mRNA from AUG and GA_{70} in DHX36 Ctrl and KD HeLa cells. NLuc mRNAs were normalized to FF mRNA and compared with DHX36 Ctrl. Data in (*D*) and (*F*) are represented as mean ± SD, n = 9 to 12. Data in (*G*) are mean ± SD, n = 3. Two-tailed Student's *t* test with Bonferroni and Welch's correction, *$p < 0.05$; **$p < 0.01$; ***$p < 0.001$; and ****$p < 0.0001$. AUG-FF, AUG-initiated firefly luciferase; Ctrl, control; DHX36, DEAH-box helicase 36; KD, knockdown; NLuc, nanoluciferase; NS, not significant; RAN, repeat-associated non-AUG.

AUG-initiated FFLuc as transfection control (Fig. 2*D* and Fig. S2*F*). C9RAN translation in the GA and GR reading frames was also selectively decreased in the DHX36 KD line with doxy induction when compared with the dimethyl sulfoxide vehicle–treated cells, suggesting that the effect was DHX36 specific (Fig. S3*A*). Either no significant transcript bias or an opposite production bias favoring DHX36 KD was observed for AUG transcripts (Fig. 2, *D* and *F*). To confirm these findings using an orthogonal readout, we performed immunoblots to detect FLAG signal on lysates from both Ctrl and DHX36 KD cells. As we had observed in our luciferase assays, DHX36 KD led to a significant decrease in the GA C9RAN-NLuc protein without impairing AUG translation of NLuc from a separate reporter (Fig. 2*E*).

To determine if loss of DHX36 might have broader effects on protein translation in these cells, we performed a surface sensing of translation assay, which measures puromycin incorporation into nascent proteins (58). Treatment with puromycin for 10 min led to a smear of proteins detectible by puromycin immunoblot. There was no difference between DHX36 Ctrl and KD cells in this assay (Fig. S2, *D* and *E*), suggesting that rates of global translation are not demonstrably affected by KD of DHX36 in these cell lines.

DHX36 depletion impairs RAN translation from CGG repeats

RAN translation occurs at multiple different GC-rich repeat sequences, some of which are capable of forming G4 structures and some of which are less likely to form such structures. We therefore evaluated whether DHX36 KD impacts RAN translation at these other repeats. Expansion of transcribed CGG repeats in the 5′UTR of *FMR1* causes fragile X–associated tremor/ataxia syndrome (59, 60). RAN translation from this repeat in the +1 reading frame generates a polyglycine protein (FMRpolyG) that accumulates within inclusions in patient brains and model systems (59, 61–64). This repeat is capable of forming either a hairpin structure or a G4 structure *in vitro* (65–68). Using an NLuc reporter with 100 repeats (+1CGG_{100}) (69), we observed that KD of DHX36 significantly suppressed CGG RAN translation of FMRpolyG on a scale comparable to that of C9RAN reporters (Fig. 2*F*). This decrease in CGG RAN translation was also evident by immunoblot (Fig. 2*E*).

We next measured reporter mRNA levels in transfected Ctrl and DHX36 KD cells. Surprisingly, we observed only a small decrease in mRNA production that was not statistically significant (Fig. 2*G*). In parallel, we also evaluated the impact of DHX36 overexpression on reporter expression. As with KD, overexpression of DHX36 did not significantly impact steady-state reporter RNA expression in HeLa cells (Fig. S5). These data suggest that the suppression of RAN translation in DHX36 KD cells is most likely a post-transcriptional event.

DHX36 KO impairs in-cell and in vitro C9RAN translation

As a second assay system in which to study the effect of DHX36, we generated a DHX36 stable KO (DHX36 KO) Jurkat cell line using a CRISPR–Cas9 targeting approach. WT Jurkat cells had no mutations at the DHX36 locus (insertion/deletion: 0/0), whereas DHX36 KO Jurkat cells (DHX36 KO) had single allele KO disruption on one allele and a 6 bp insertion on the other allele at the target site (insertion/deletion: +5/+6) (Fig. S4, *A* and *B*). Western blot analysis showed elimination of full-length DHX36 protein in Jurkat DHX36 KO cell lines (Fig. 3*A*). Jurkat DHX36 KO cells exhibited impaired RAN translation across all three potential G_4C_2 reading frames, similar to what we observed in HeLa DHX36 KD cells (Fig. 3*B*).

The effects of DHX36 KD on RAN translation product generation could theoretically be elicited by changes in RNA or protein stability or by actively impacting protein translation. To investigate this question, we utilized an *in vitro* translation assay using lysates derived from DHX36 WT or KO Jurkat cells. Previous studies in similar conditions demonstrated that we could accurately measure C9RAN translation in this context and that production from our RAN reporters is not dependent on mRNA or reporter stability (29, 69). We harvested Jurkat DHX36 WT and KO cell lysates, added AUG- or G_4C_2-repeat RNA in GA (+0) frame and *in vitro* translated for 2 h (Fig. 4*C* and Fig. S4*C*). AUG-NLuc translation from DHX36 KO lysates was consistently lower than that from WT Jurkat lysates. However, this effect was much larger for GA-NLuc reporters, which exhibited 36% as efficient a translation in DHX36 KO lysates compared with WT lysates over in more than four independent experiments (Fig. S4*C*). Together, these results suggest that loss of DHX36 suppresses RAN translation from G_4C_2 repeats in multiple reading frames of G_4C_2 repeats and is mainly acting at the level of translation.

The effect of DHX36 on C9RAN translation is dependent on repeat length

Translation of C9RAN reporters in the GA reading frame initiates primarily from an upstream CUG start codon that supports translation even at small repeat sizes (29, 31, 32, 70). If DHX36 contributes to RAN translation by resolving G4 structures, then we would predict that the loss of DHX36 would selectively reduce translation for transcripts with larger repeats. In HeLa cells, expression of C9 GA frame reporters with 3×, 35×, and 70× G_4C_2 repeats was selectively suppressed by DHX36 loss at the larger repeat sizes (Fig. 4, *A* and *B* and Fig. S3*B*). Similar results were observed in Jurkat DHX36 stable KO cells (Fig. 4*C*). These results suggest that loss of DHX36 selectively acts to reduce C9RAN translation in a repeat length–dependent manner.

The effect of DHX36 overexpression on C9RAN DPR expression

Since depletion of DHX36 results in a significant decrease in C9RAN translation, we wondered if overexpression of DHX36 enhances C9RAN. To address this, we expressed either a DHX36 WT or a DHX36-E335A mutant, which lacks the helicase activity required to unwind G4 structures in parental HeLa cells. To ascertain the impact of DHX36 on translation in particular, we conducted studies using transfected *in vitro*–transcribed C9RAN reporter mRNAs. In HeLa cells, overexpression of DHX36 significantly increased C9RAN from

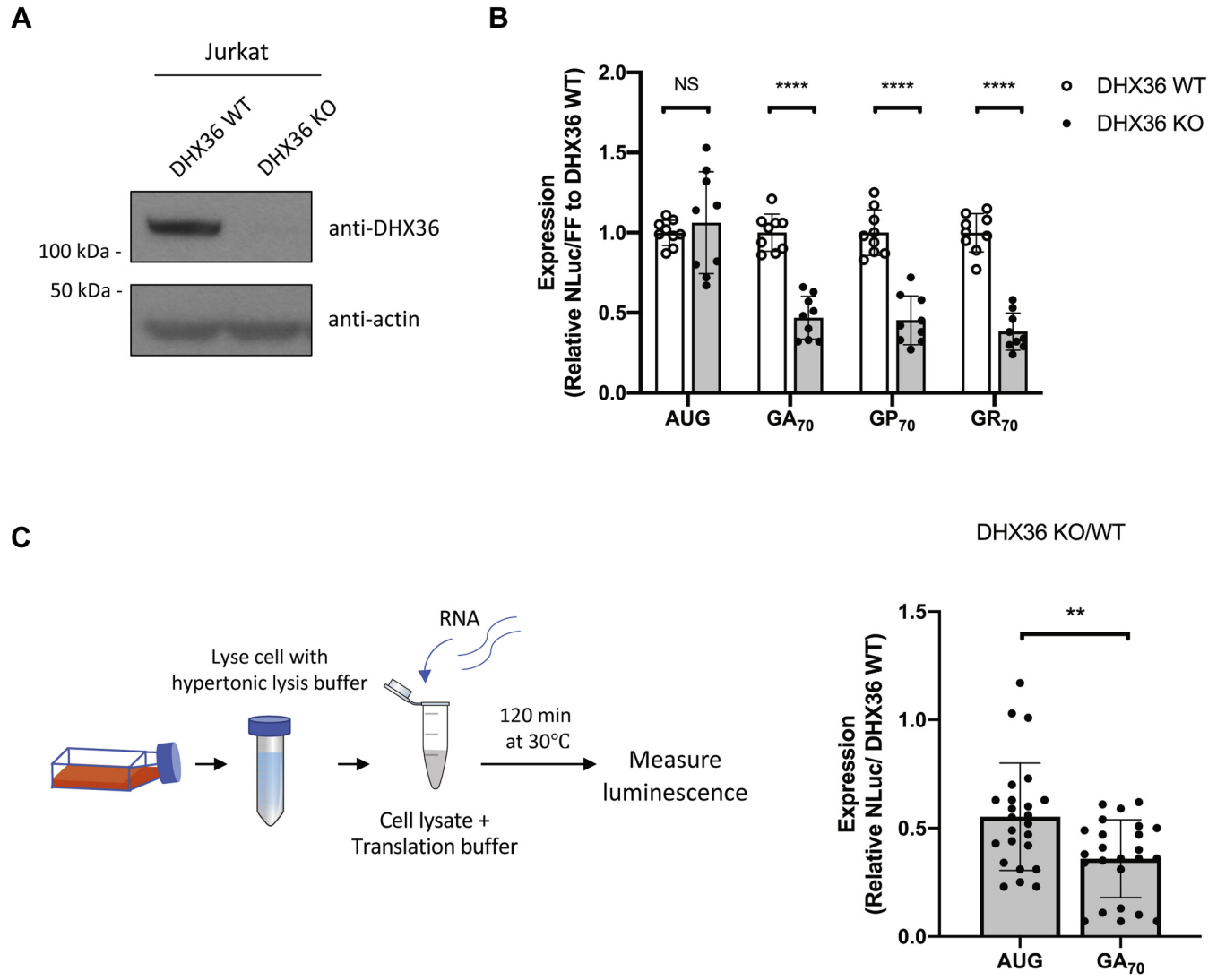

Figure 3. C9RAN reporter expression in DHX36 KO Jurkat cell lines and *in vitro* cell lysates. *A*, immunoblots to DHX36 from WT and DHX36 KO Jurkat cells. *B*, relative expression of AUG and C9-RAN translation from GA (+0), GP (+1), and GR (+2) reading frames in WT and DHX36 KO Jurkat cells. NLuc signal were normalized to AUG-FF and compared between WT and DHX36 KO Jurkat cells. Data are represented as mean ± SD, n = 9. *C*, *in vitro* translation using lysates derived from DHX36 WT and KO Jurkat cells for AUG-NLuc RNA and C9-RAN in GA frame RNA. NLuc signals were normalized to signal from DHX36 WT. Data are represented as mean ± SD, n = 24. Two-tailed Student's *t* test with Bonferroni and Welch's correction, $*p < 0.05$; $***p < 0.001$; and $****p < 0.0001$. AUG-FF, AUG-initiated firefly luciferase; DHX36, DEAH-box helicase 36; NLuc, nanoluciferase; RAN, repeat-associated non-AUG.

transfected reporter RNAs in all three sense reading frames. This effect was specific to DHX36 WT, as DHX36-E335A has no effect on C9RAN DPR production when normalized to the FFLuc mRNA reporters, and Western blot analysis confirmed this relationship (Fig. 5). These data suggest that DHX36 acts post-transcriptionally to enhance RAN translation.

KD of DHX36 prevents stress-dependent upregulation of RAN translation

Activation of the integrated stress response (ISR), which triggers phosphorylation of eukaryotic translation initiation factor 2 subunit alpha and formation of SGs, suppresses global protein translation initiation by impairing ternary complex recycling (71–75). Paradoxically, ISR activation enhances RAN translation from both CGG and G_4C_2 repeats, and repeat expression in isolation can trigger SG formation (29, 30, 32, 37). Loss of DHX36 induces spontaneous SG formation, suggesting that DHX36 may play a role in G4 structure–induced cellular stress (53). We therefore wondered what impact loss of DHX36 would have on regulation of RAN translation in the setting of ISR activation. We cotransfected C9-NLuc and FFLuc into DHX36 Ctrl or DHX36 KD HeLa cells and then treated them with 2 μm of the endoplasmic reticulum stress inducer thapsigargin (Tg) for 5 h. Tg treatment decreased expression of FFLuc in both Ctrl cells and in DHX36 KD cells, which is consistent with appropriate activation of the ISR in these cells (Fig. 6*A*, *right*). Consistent with prior studies (29, 37), Tg treatment in DHX36 Ctrl cells elevated C9RAN reporter levels compared with dimethyl sulfoxide treatment. However, depletion of DHX36 precluded this upregulation in

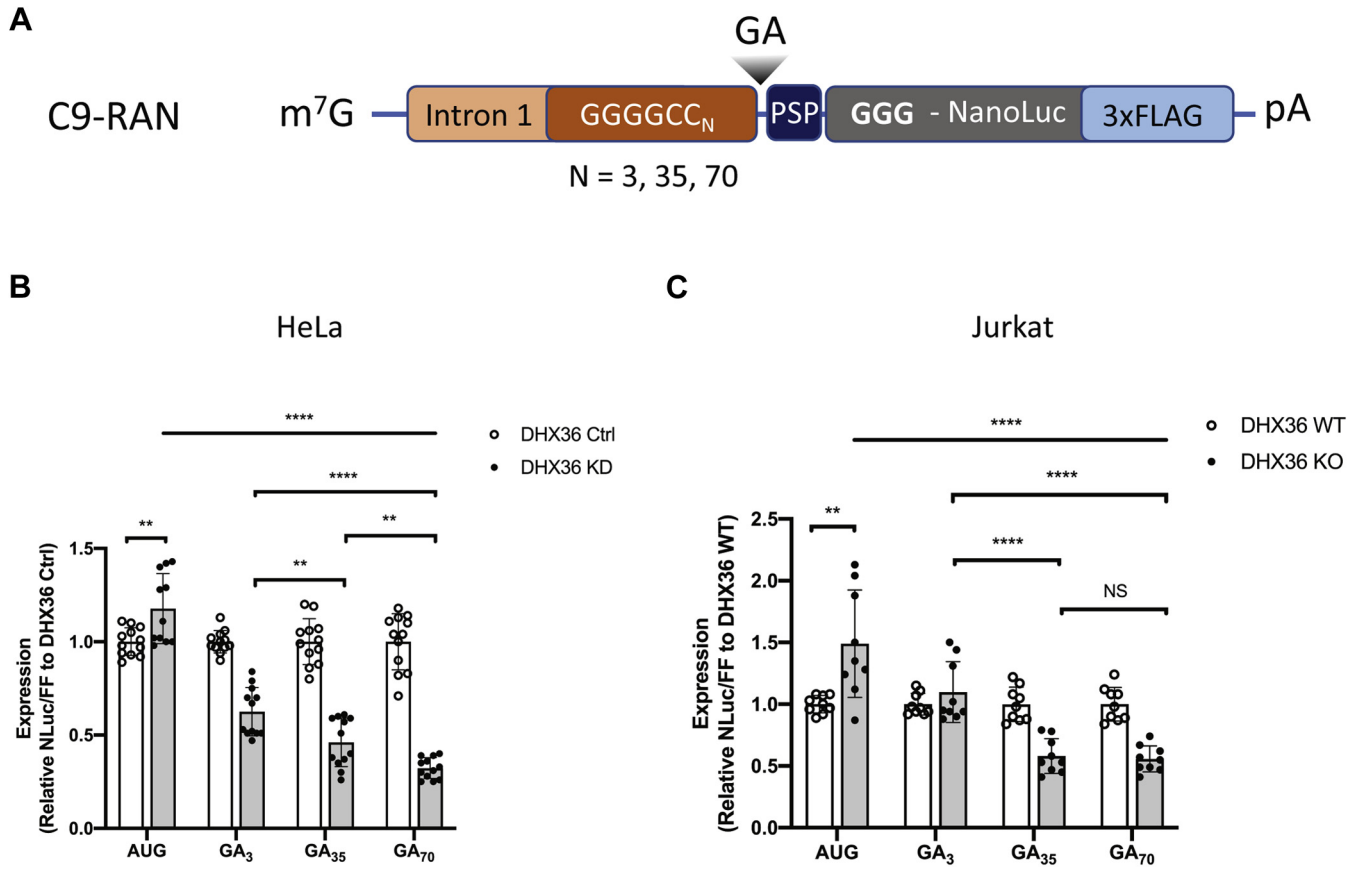

Figure 4. The effect of decreased DHX36 on C9RAN reporter expression is G_4C_2 repeat length dependent. *A*, schematic of previously published luciferase reporters of C9-RAN in GA frame harboring different repeat sizes. *B* and *C*, relative expression of AUG and C9-RAN translation from GA frames with 3, 35, and 70 repeats in Ctrl and DHX36 KD HeLa cells (*B*) and DHX36 WT and KO Jurkat cells. NLuc signals were normalized to AUG-FF. Data are represented as mean ± SD, n = 9 to 12. One-way ANOVAs were performed to compare the statistical differences between repeat length in DHX36 KD or KO cell lines. Two-tailed Student's *t* test with Bonferroni and Welch's correction were then performed to confirm the differences between multiple comparison, $*p < 0.05$; $**p < 0.01$; and $****p < 0.0001$. AUG-FF, AUG-initiated firefly luciferase; Ctrl, control; DHX36, DEAH-box helicase 36; G_4C_2, GGGGCC; KD, knockdown; NLuc, nanoluciferase; RAN, repeat-associated non-AUG.

C9RAN by Tg (Fig. 6*A*). Similar findings were also observed by immunoblot in studies where we cotransfected the C9RAN reporters and GFP as a control for transfection and AUG initiated translation (Fig. 6*B*). These data suggest that DHX36 may play a role in regulating the stress induction of RAN translation induced by the ISR.

Discussion

DNA and RNA G4 structures strongly influence both gene transcription and mRNA stability, localization, and translation. Moreover, G4 structures are implicated in a number of human disorders, including C9 FTD/ALS (76, 77). Here we find that a major human G4 helicase, DHX36, enhances C9RAN translation from expanded G_4C_2-repeat reporter RNAs in human cells. These effects on RAN translation require DHX36 helicase activity on G4 RNA. DHX36 is also required for efficient C9RAN and CGG RAN translation as KD or KO of DHX36 in human cells suppressed RAN translation from both G_4C_2 and CGG repeats. We also observe a robust suppression of *in vitro* C9RAN translation in DHX36 KO cell–derived lysates. Overall, these data are consistent with a model whereby DHX36 binds to and unwinds GC-rich repeat RNA structures and enhances their non-AUG–initiated translation with a potential secondary role in enhancing repeat transcription (Fig. 7).

The observed effects on C9RAN reporter generation are largely post-transcriptional. While we do observe a stimulatory effect of DHX36 on T7 polymerase transcription from a C9-repeat *in vitro* (Fig. 1, *D* and *E*), we do not observe changes in C9-repeat RNA levels in cells following DHX36 KD or overexpression (Fig. 2*G* and Fig. S5). We also show that DHX36 directly binds to C9-repeat DNA with a binding affinity of ~10 to 100 less than previously reported for pure G4 DNAs (40, 47, 52) (Fig. 1, *A*–*C*). The relatively low affinity of DHX36 for C9-repeat G4 DNA might in part explain the lack of a robust effect on C9-repeat transcript levels in cells following DHX36 KD or overexpression. In addition, T7 polymerase *in vitro* is prone to early transcription termination (78) and as such may be less efficient than RNA polymerase complexes at resolving RNA structures and generating complete transcripts in cells. Future work using patient-derived cells harboring greater repeat lengths (which DHX36 may have greater affinity for) will be necessary to more fully characterize the potential for DHX36 to modulate C9-repeat transcription in patients.

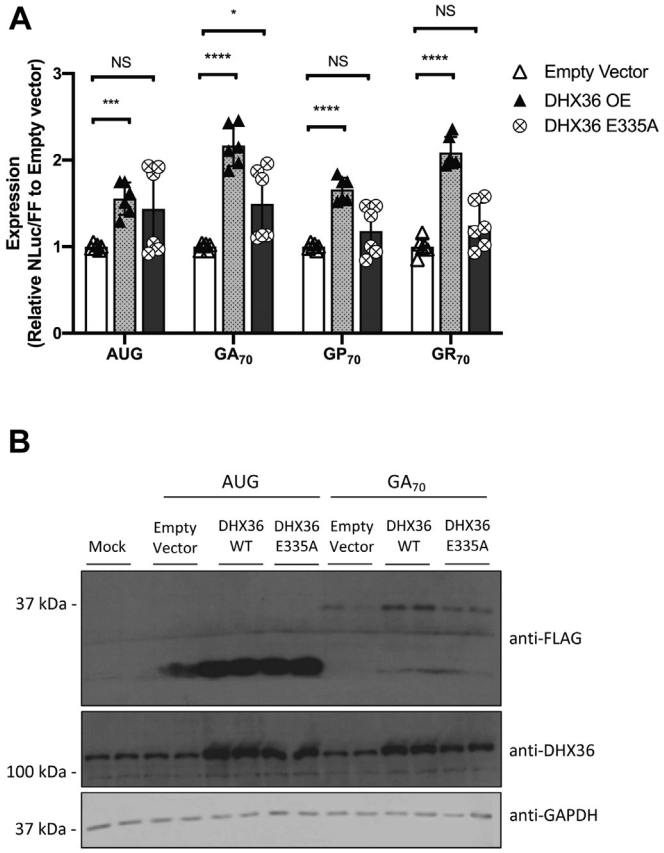

Figure 5. DHX36 overexpression enhances C9RAN reporter expression from G_4C_2 repeat RNA. *A*, relative expression of AUG and C9-RAN translation when cotransfecting reporter RNA and overexpression of empty vector, WT, or E335A DHX36 DNA plasmids in HeLa cells. Data are represented as mean ± SD, n = 9. Two-tailed Student's *t* test with Bonferroni and Welch's correction, $*p < 0.05$; $***p < 0.001$; and $****p < 0.0001$. *B*, Western blot analysis of cotransfected AUG and C9-RAN luciferase reporters in RNA and empty vector, DHX36 WT, or DHX36 E335A DNA plasmids in HeLa cells. GAPDH was blotted as internal control. DHX36, DEAH-box helicase 36; G_4C_2, GGGGCC; RAN, repeat-associated non-AUG.

DHX36 binds to C9-repeat RNA in a G4-specific manner both *in vitro* and in studies using human cell and mouse spinal cord lysates (6, 49, 79). Depletion of DHX36 decreases C9RAN translation, and this decrease occurs across all reading frames and is dependent on the length of the repeats (Figs. 2–4). In addition, while this article was in revision stage, a second study was published where similar effects of DHX36 were observed on C9RAN translation (80). We further observe similar results for CGG repeats capable of supporting RAN translation and folding into G4 structures. This suggests that RAN translation initiation or elongation could be significantly influenced by both RNA-binding protein recognition and resolution of repeat RNA secondary structures. This idea is supported by the finding that a helicase dead form of DHX36 failed to influence RAN translation of C9-repeat RNAs. It is also consistent with prior studies implicating RNA helicases such as DDX3X and the eukaryotic translation initiation factor 4A helicase cofactors eukaryotic translation initiation factor 4B and eukaryotic translation initiation factor 4H as modifiers of RAN translation at both CGG and G_4C_2 repeats (33, 36).

In addition, depletion of DHX36 precluded the augmentation of RAN translation typically observed in response to stress (Fig. 6) (29, 30, 81). DHX36 is a component of SGs and plays an active role in regulating the cellular stress response (82–84). Indeed, KD or KO of DHX36 is sufficient to trigger SG formation without application of an exogenous stressor (53). How exactly loss of DHX36 precludes this upregulation is not clear. ISR activation augments RAN translation at least in part by lowering initiation codon fidelity requirements (29, 31). If DHX36 is specifically influencing elongation through the repeat, then its depletion may slow translation because of ribosomal stalling within the repeats despite continued enhanced initiation. Alternatively, G_4C_2 repeats also support a 5′ M^7G cap–independent "IRES-like" RAN initiation mechanism that is enhanced by ISR activation (30, 85–87). DHX36 could play an active role in generating this structure and allowing for internal ribosome entry. A deeper understanding of RNA structure–function relationships as they apply to RAN translation will be needed to determine which of these mechanisms (or both) is likely to explain how DHX36 loss impacts RAN translation at both CGG and G_4C_2 repeats.

This study has some limitations. It largely relies on reporter assays using transiently transfected plasmids or *in vitro*–transcribed linear RNA. RAN translation from the endogenous locus of C9 might involve very large RNA from longer repeats, and the exact nature of the RAN-translated transcripts in C9 patient neurons remains unclear. In particular, endogenous RNAs may form a combination of dynamic secondary structures including hairpins and G4s, which complicate the potential effects on both RNA-mediated toxicity and RAN translation. Further studies using endogenous systems such as C9 FTD/ALS patient induced pluripotent stem cell–derived neurons and rodent that harbor larger repeats will be needed to confirm the roles of DHX36 in endogenous repeat transcription, RAN translation, and toxicity derived from the endogenous repeat.

In sum, this study provides evidence that DHX36 can influence RAN translation of G_4C_2 repeats both basally and in response to stress pathways. These studies suggest that control of G4 formation at the DNA and RNA levels and modulation of G4-resolving helicases such as DHX36 are candidate therapeutic strategies and targets for G-rich repeat–associated neurological diseases.

Experimental procedures

EMSAs

About 62.5 pg of 5′-IRDye 800–labeled C9 or scrambled oligonucleotides (Table 1) were synthesized (Integrated DNA Technologies, Inc) and heated in nuclease-free water in the presence of KCl (100 mM) starting at 98 °C and decreasing 10 °C every 2 min, ending at 28 °C. As a control, 62.5 pg of C9 oligonucleotides were heated and cooled as aforementioned in the absence of KCl, 3.75 pg of each oligonucleotide were incubated at 37 °C for 30 min in binding buffer (143 mM EDTA) with varying concentrations of rDHX36 (7.4, 4.5, 1.7, 1.1, or 0 nM). Additional

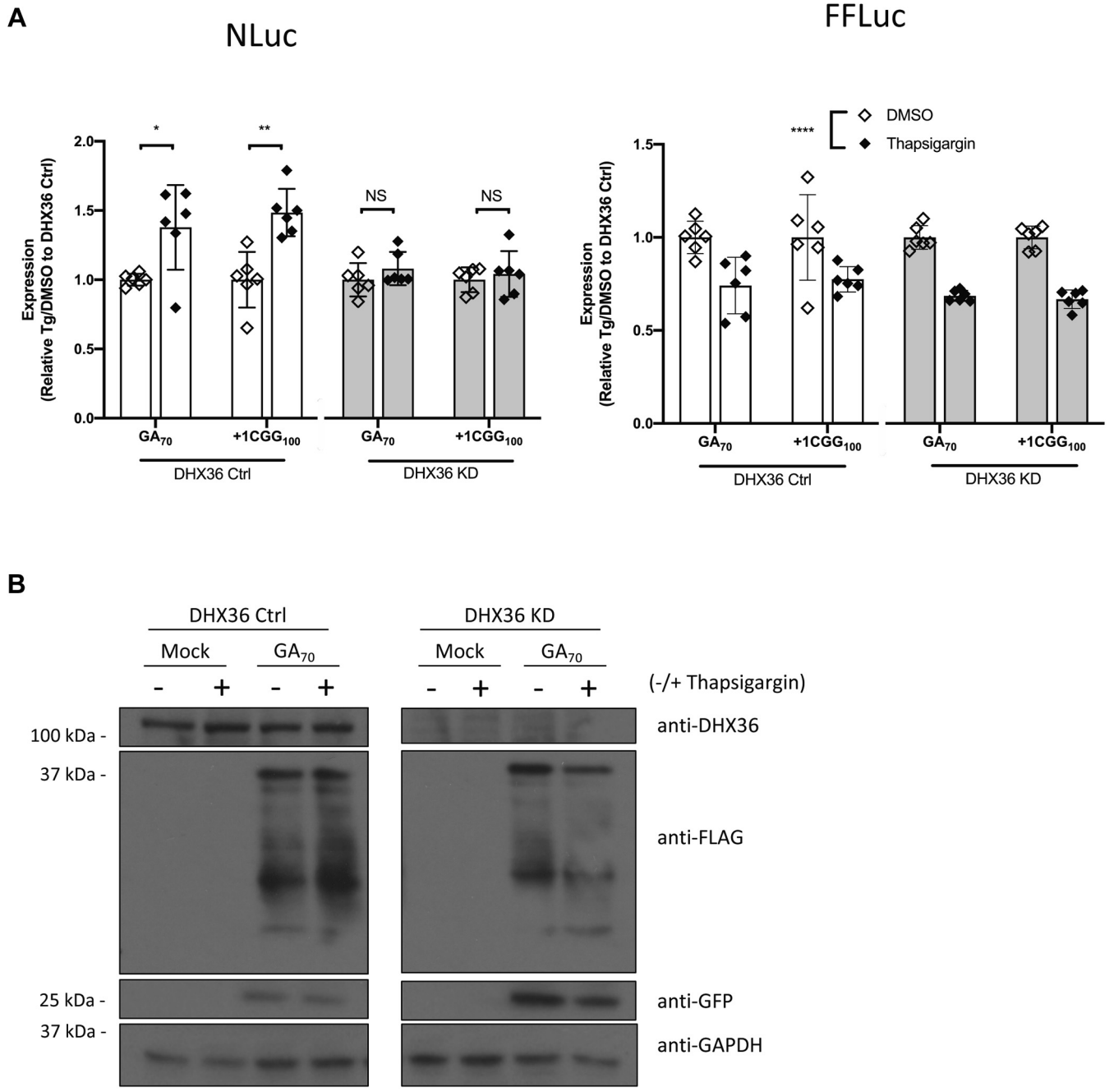

Figure 6. KD of DHX36 prevents stress-dependent upregulation of C9RAN reporter expression. *A*, relative expression of RAN translation in G_4C_2 and CGG repeat treated with 2 μM thapsigargin (Tg) or DMSO in Ctrl and DHX36 KD HeLa cells. NLuc (*left*) and FF (*right*) signals were represented as ratio of Tg-treated cells to DMSO-treated cells and compared between Ctrl and DHX36 KD HeLa cells. *B*, immunoblots of G_4C_2 and CGG RAN luciferase reporters in Ctrl and DHX36 KD HeLa cells treated with 2 μM Tg. GFP was blotted as a transfection Ctrl, and GAPDH was blotted as internal Ctrl. For panel *A*, data are represented as mean ± SD, n = 6. Two-way ANOVA was performed to discern effect of Tg treatment across cell types. Two-tailed Student's *t* test with Bonferroni and Welch's correction was performed to assess differences between individual groups. *$p < 0.05$; **$p < 0.01$; and ****$p < 0.0001$. Ctrl, control; DHX36, DEAH-box helicase 36; DMSO, dimethyl sulfoxide; G_4C_2, GGGGCC; KD, knockdown; NLuc, nanoluciferase; RAN, repeat-associated non-AUG.

volumes of buffer (75 mM Tris–acetate, pH 7.8, 75 mM NaCl, 3.03 mM $MgCl_2$, 15.2% glycerol, 0.02% lactalbumin, 21.7 mM 2-mercaptoethanol, 7.58× protease inhibitor cocktail [Roche], and 0.04 μg/μl leupeptin) were added to the 4.5, 1.7, 1.1, or 0 nM reactions so as to have equal buffer concentrations in all reactions. Glycerol (16% final) was added to the samples, and 3 pg of DNA were loaded per well onto a 10% nondenaturing PAGE. The samples were electrophoresed for 5 h at 120 V in the dark. Each EMSA was performed in triplicate and analyzed using a Odyssey Imager (Li-Cor). Percent bound was determined by densitometry measurements in ImageStudio using the following equation: percent bound = (bound DNA/total DNA) × 100. Triplicate values were averaged and plotted with Prism 8.3.1 (Graphpad) using a nonlinear regression (curve fit) function.

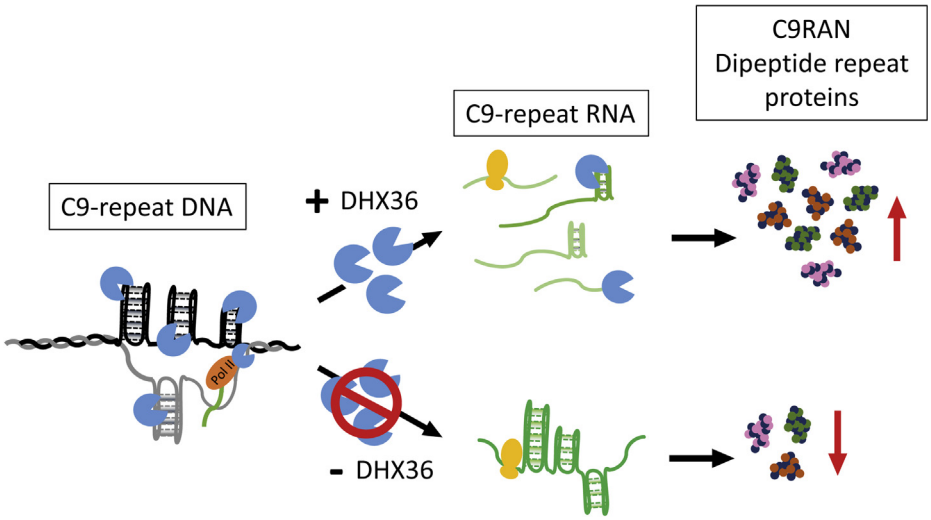

Figure 7. Model of DHX36 modulation of C9RAN translation. DHX36 binds to G-quadruplex DNA and RNA structures. DHX36 aids transcription through large stretches of G_4C_2-repeat RNA *in vitro*, but its effects in human cells with large repeats are unclear. Depletion of DHX36 decreases RAN translation from both CGG- and C9-repeat reporters—both of which are capable of forming G-quadruplex structures–whereas increased DHX36 expression enhances C9RAN translation. These findings suggest a direct role for DHX36 in RAN translation of GC-rich repeats. DHX36, DEAH-box helicase 36; G_4C_2, GGGGCC; RAN, repeat-associated non-AUG.

In vitro *transcription assay*

A HiScribe T7 Quick High Yield RNA Synthesis Kit (New England Bio Labs; catalog no. E2050S) was used with 0.5 μg of a GA_{70} or AUG-NLuc linearized plasmid as template (29). The reactions were transcribed overnight at 37 °C in the presence or the absence of DHX36 (0 or 6 nM). An additional volume of DHX36 storage buffer was added to reactions without DHX36 so as to have equal buffer concentrations in all reactions. The resulting transcripts were treated with DNase for 20 min at 37 °C and then isolated using Micro Bio-Spin 6 Columns (Bio-Rad Laboratories, Inc; catalog no. 732-6221). About 0.75 μg of RNA transcripts were mixed with 2× formamide buffer (95% deionized formamide, 0.025% bromophenol blue, and 5 mM EDTA) and heated at 95 °C for 5 min. The samples were resolved in a 7.5% denaturing-8 M urea PAGE for 20 min at 2 W and then 3 h at 20 W. The gels were subsequently soaked in SYBR gold nucleic acid stains (Thermo Fisher Scientific; catalog no. S11494) for 20 min at room temperature and imaged using a Bio-Rad Gel Docs XR+ system and quantified using densitometry software. Densitometry values for the top third of the gel were divided by total value for each lane. Values for total densitometry readings for each lane were also taken.

RNA synthesis

pcDNA3.1(+)/NLuc-3xF and pcDNA3.1(+)/FF were linearized by PspOMI and XbaI restriction enzymes, respectively, and recovered using DNA Clean and Concentrator-25 kits (Zymo Research; catalog no. D4033). m^7G-capped and polyadenylated RNAs were transcribed *in vitro* from these plasmids using HiScribe T7 ARCA mRNA Kit, with polyA tailing (NEB; catalog no. E2065S) following the manufacturer's instructions and recovered using RNA Clean and Concentrator-25 kits (Zymo Research; catalog no. R1017). The integrity and size of all transcribed RNAs were confirmed by denaturing formaldehyde and formamide agarose gel electrophoresis.

Cell culture, transfection, quantitative RT-PCR, and drug treatment

Jurkat T1-28/11 and HeLa 15/25 cells were cultured and passaged at 37 °C, 5% CO_2. Jurkat T1-28/11 cells were maintained in RPMI 1640 medium supplemented with 10% fetal bovine serum. HeLa 15/25 cells were maintained in Dulbecco's modified Eagle's medium supplemented with 10% fetal bovine serum, 1% nonessential amino acids, 3 μg/ml blasticidine, and 250 μg/ml zeocin. To induce DHX36 KD, HeLa 15 and HeLa 25 were both treated with daily changed media containing 1 μg/ml doxy for 4 days.

For transfection and luciferase assay in Jurkat cells, cells were plated in 24-well plates at 6×10^5 cells/well in 500 μl media. Reverse transfection by using TransIT-Jurkat transfection reagent (Mirus; catalog no. MIR 2124) was done after plating of cells. Cells were cotransfected with 250 ng/well of pcDNA(+)-NLuc-3xFLAG plasmids developed from Green *et al.* (29) and Kearse *et al.* (69) and 250 ng/well of pGL4.13 FFLuc plasmid as a transfection control. Mixed plasmids and reagents were added dropwise in cultured cells after 30 min incubation at room temperature, and then the plate was gently shaken for 1 min. Luciferase assays were performed 48 h after

Table 1
DNA oligonucleotides used in this study

Oligonucleotide name	5′ label	Sequence (5′-3′)
$(G_4C_2)_5$-DNA	IRDye 800	GGGGCCGGGGCCGGGG CCGGGGCCGGGGCCG TTAGAATTTTT
Scrambled	IRDye 800	GCGAGTGCGAGAGCGTG TGCGCGCGTGCGCGAGCG CGTGTGT

plasmid transfection. Cells from each well were collected in microcentrifuge tube, and media were removed after 400 rpm centrifugation for 5 min. Then cells from each tube were lysed with 60 μl of Glo Lysis Buffer 1× (Promega; catalog no. E2661) and were vortexed for 5 s. In opaque white 96-well plates, from 60 μl of cell lysate, 25 μl of cell lysate was distributed to mix with 25 μl of Nano-Glo Luciferase Assay System (Promega; catalog no. N1120), and another 25 μl of cell lysate was mixed with 25 μl of ONE-Glo Luciferase Assay System (Promega; catalog no. E6130). The plate was placed on a shaker for 5 min in the dark. Luciferase activity in each well was obtained by luminescence measurements. All reagents and experiments are presented at room temperature.

For transfection and luciferase assay in HeLa cells, cells were plated in 96-well plates at 2.5×10^5 cells/well in 100 μl media. About 24 h after plating, cells were cotransfected with 50 ng/well of pcDNA(+)-NLuc-3xFLAG plasmids and 50 ng/well of pGL4.13 FFLuc plasmid as transfection control. Transfection was done by adding Viafect transfection reagent (Promega; catalog no. E4981) with mixed plasmids dropwise in cultured cells after 10 min of incubation at room temperature and then gently shaking the plate for 1 min. Plasmid DNA and C9-repeat RNA cotransfection were done by forward transfection of published DNA plasmid expressing empty vector, WT, or E335A DHX36 (41) in HeLa cells seeded at 2.5×10^5 cells/well in 100 μl media. After 24 h, *in vitro*–synthesized C9-RNA and pcDNA-FF RNA were cotransfected at 50 ng/well each into the well by Viafect transfection reagent (Promega; catalog no. E4981) as described previously. Following luciferase assays were performed 24 h after C9-repeat DNA plasmids or RNA transfection, as described by Kearse *et al.* (69).

For quantitative RT-PCR assays, after HeLa cells were plated and transfected as described previously, experiments were performed as described by Linsalata *et al.* (33).

For C9RAN reporter luciferase analysis following stress activation, after 4 days of doxy treatment in HeLa 15/25 cells, cells were seeded and transfected for 19 h and then followed by 5 h treatment of 2 μM Tg.

Immunoblot and antibodies

In a 12-well plate, HeLa 15/25 cells were rinsed with 500 μl cold 1× PBS twice and then lysed in 300 μl radioimmunoprecipitation buffer with protease inhibitor (120 μl for 24-well plates) for 30 min at a 4 °C shaker. Lysates were homogenized by passing through a 28-gauge syringe eight times, mixed with 6× sample buffer with a final of 2% beta mercaptoethanol (β-ME), denatured at 95 °C for 10 min, and stored at −20 °C. Protein samples were standardized by bicinchoninic acid assay for equal total protein loading. About 20 μl of equal total protein sample was loaded in each well of a 10% SDS-PAGE. All primary antibodies applied for Western blot were used at 1:1000 dilution in 5% nonfat dairy milk (w/v) and 0.1% Tween-20 (v/v) in Tris-buffered saline except antipuromycin at 1:5000 dilution. Monoclonal mouse anti-DHX36 antibody was generated at 2.57 μg/μl (41), monoclonal mouse anti-FLAG antibody was from Sigma (clone M2; catalog no. F1804), mouse anti-GFP was from Roche (catalog no. 11814460001), monoclonal mouse anti-GAPDH was from Santa Cruz Biotechnology (clone 6C5; catalog no. sc-32233), and mouse antipuromycin 12D10 was from Millipore (catalog no. MABE434).

Jurkat cell line generation

The DHX36 guide RNAs (T1, T2, and T10) were designed to target exonic regions of DHX36–G4R1 (gene ID: 170506) in order to disrupt all the gene products (Fig. S3). The guide RNA T1 (AAGTACGATATGACTAACAC) was evaluated to be the most effective by nucleotide mismatching assay in the cell pool examination (31.2% cleavage efficiency) and was utilized for generation of single cell clones. Cleavage efficiency was determined by sequencing trace analysis with the online tool TIDE (https://tide-calculator.nki.nl/). Clones were identified and confirmed using Sanger Sequencing of PCR and RT-PCR productions (Fig. S3) and Western blot analysis (Fig. 3*A*).

In vitro *translation assays*

Preparation of cell lysate, hypertonic lysis buffer, and translation buffer were followed by Linsalata *et al.* (33). Jurkat cells were centrifuged and rinsed three times with PBS (pH 7.4). Hypotonic lysis buffer that contained 10 mM Hepes–KOH (pH 7.6), 10 mM KOAc, 0.5 mM Mg2OAc, 5 mM DTT, and EDTA-free protease inhibitor was added to cells pellet on ice to swollen the cells for 30 min. Then cells were mechanically lysed by 20 strokes in a 27-gauge syringe and followed by another 30 min of incubation on ice. The supernatant from the cell lysate was collected by centrifuging the cell lysate at 10,000*g* for 10 min at 4 °C and further diluted in lysis buffer to 8.0 μg/μl using a modified Bradford protein quantification assay (Bio-Rad), flash frozen in liquid nitrogen, and stored at 80 °C. The lysates were added to the translation buffer with final concentrations of 20 mM Hepes–KOH (pH 7.6), 44 mM KOAc, 2.2 mM Mg2AOc, 2 mM DTT, 20 mM creatine phosphate (Roche), 0.1 μg/μl creatine kinase (Roche), 0.1 mM spermidine, and on average 0.1 mM of each amino acid.

For *in vitro* translation assays, 40 fmol of RNA was added to lysate with protein concentration at 8 μg/μl of 10 μl per reaction. After incubation at 30 °C for 120 min, 25 μl of Glo Lysis Buffer (Promega) was added to the reaction to incubate for 5 min at room temperature. With the Nano-Glo Dual-Luciferase System, 25 μl of this mixture was added, and 25 μl of the ONE-Glo EX reagent following 25 μl of NanoDLR Stop & Glo reagent (Promega) was added. All mixtures were incubated in opaque white 96-well plates on a rocking shaker in the dark for 5 min before quantifying the luminescence.

Measuring protein synthesis by puromycin incorporation

Nascent global translation was monitored by the surface sensing of translation method (58). After seeding HeLa cells as described previously in a 24-well plate format, 48 h later, cells were incubated with fresh media containing 10 μg/ml of puromycin for 10 min at room temperature. Cells were then

placed on ice and washed with ice-cold PBS, prior to lysis in 100 µl radioimmunoprecipitation buffer containing protease inhibitor.

Statistical methods

Statistical analysis was performed using GraphPad Prism 8. For comparison of NLuc and FFLuc reporter luciferase activity, one-way ANOVAs were performed to confirm statistical difference between Ctrl and experimental groups. Two-way ANOVA was performed to confirm the statistical difference on FFLuc signal from the treatment of Tg between different groups of Ctrl and experimental conditions. Post hoc Student's *t* tests were then performed with Bonferroni correction for multiple comparisons and Welch's correction for unequal variance. All studies represent at least three independently replicated experiments. All bar graphs include a standard deviation error bar and each independent replicate. Exact N for each sample and analysis performed are noted in the legend to the figure.

Data availability

All data for this study are contained within this article.

Supporting information—This article contains supporting information including uncropped gel and blot images (Figs. S6 and S7).

Acknowledgments—We thank everyone in the Todd laboratory and the Smaldino laboratory for thoughtful feedback and discussion on this project. Jiou Wang provided initial G_4C_2 repeat plasmids to the Smaldino laboratory.

Author contributions—Y.-J. T., S. N. S., P. K. T., and P. J. S. formal analysis; Y.-J. T. and M. A. R. validation; Y.-J. T., S. N. S., K. M. G., A. E. C., A. K., M. E. S., M. A. R., A. E. R., J. P. V., P. K. T., and P. J. S. investigation; Y.-J. T. and S. N. S. visualization; Y.-J. T., S. N. S., A. E. C., A. E. R., M. A. S., Y.-H. W., P. K. T., and P. J. S. methodology; Y.-J. T., P. K. T., and P. J. S. writing–original draft; Y.-J. T., S. N. S., A. E. C., H. M. R., M. E. S., A. E. R., E. D. R., Y.-H. W., J. P. V., P. K. T., and P. J. S. writing–review and editing; K. M. G., A. E. C., A. K., H. M. R., E. D. R., M. A. S., Y.-H. W., J. P. V., P. K. T., and P. J. S. conceptualization; K. M. G., A. E. R., M. A. S., P. K. T., and P. J. S. supervision; A. K., E. D. R., P. K. T., and P. J. S. resources; M. A. S., Y.-H. W., J. P. V., P. K. T., and P. J. S. funding acquisition; Y.-H. W., P. K. T., and P. J. S. project administration.

Funding and additional information—This work was funded by the National Institutes of Health (R15 AG067291 to P. J. S., T32GM008136 to H. M. R., RO1GM101192 to Y.-H. W., P50HD104463, R01NS099280, and R01NS086810 to P. K. T.), VA (BLRD BX004842 and BX003231 to P. K. T.), the University of Michigan (Cellular and Molecular Biology Graduate program and the Chia-Lun Lo Fellowship to Y.-J. T.), Ball State University (Startup Funds and Junior Faculty ASPIRE grant to P. J. S., Graduate Student ASPIRE grant to A. E. R.), and Amyotrophic Lateral Sclerosis Association grant 18-IIA-406 to P. J. S. The content is solely the responsibility of the authors and does not necessarily represent the official views of the National Institutes of Health.

Conflict of interest—P. K. T. served as a paid consultant for Denali Therapeutics, holds a joint patent with Ionis Therapeutics, and receives publishing royalties from UpToDate. None of these are directly relevant to his role on this article, and none of these organizations have any role in the conception, preparation, or editing of this article. All other authors declare that they have no conflicts of interest with the contents of this article.

Abbreviations—The abbreviations used are: C9-NLuc, C9RAN translation–specific NLuc reporter; Ctrl, control; DHX36, DEAH-box helicase 36; doxy, doxycycline; DPR, dipeptide repeat protein; FFLuc, firefly luciferase; FTD, frontal temporal dementia; G4, G-quadruplex; G_4C_2, GGGGCC; HRE, hexanucleotide repeat expansion; ISR, integrated stress response; KCl, potassium chloride; KD, knockdown; NLuc, nanoluciferase; RAN, repeat-associated non-AUG; rDHX36, recombinant DHX36; SG, stress granule; Tg, thapsigargin.

References

1. Renton, A. E., Majounie, E., Waite, A., Simón-Sánchez, J., Rollinson, S., Gibbs, J. R., Schymick, J. C., Laaksovirta, H., van Swieten, J. C., Myllykangas, L., Kalimo, H., Paetau, A., Abramzon, Y., Remes, A. M., Kaganovich, A., *et al.* (2011) A hexanucleotide repeat expansion in C9ORF72 is the cause of chromosome 9p21-linked ALS-FTD. *Neuron* **72**, 257–268
2. DeJesus-Hernandez, M., Mackenzie, I. R., Boeve, B. F., Boxer, A. L., Baker, M., Rutherford, N. J., Nicholson, A. M., Finch, N. A., Flynn, H., Adamson, J., Kouri, N., Wojtas, A., Sengdy, P., Hsiung, G. Y., Karydas, A., *et al.* (2011) Expanded GGGGCC hexanucleotide repeat in noncoding region of C9ORF72 causes chromosome 9p-linked FTD and ALS. *Neuron* **72**, 245–256
3. Van Mossevelde, S., van der Zee, J., Cruts, M., and Van Broeckhoven, C. (2017) Relationship between C9orf72 repeat size and clinical phenotype. *Curr. Opin. Genet. Dev.* **44**, 117–124
4. Byrne, S., Heverin, M., Elamin, M., Walsh, C., and Hardiman, O. (2014) Intermediate repeat expansion length in C9orf72 may be pathological in amyotrophic lateral sclerosis. *Amyotroph. Lateral Scler. Frontotemporal Degener.* **15**, 148–150
5. Umoh, M. E., Fournier, C., Li, Y., Polak, M., Shaw, L., Landers, J. E., Hu, W., Gearing, M., and Glass, J. D. (2016) Comparative analysis of C9orf72 and sporadic disease in an ALS clinic population. *Neurology* **87**, 1024–1030
6. Haeusler, A. R., Donnelly, C. J., Periz, G., Simko, E. A., Shaw, P. G., Kim, M. S., Maragakis, N. J., Troncoso, J. C., Pandey, A., Sattler, R., Rothstein, J. D., and Wang, J. (2014) C9orf72 nucleotide repeat structures initiate molecular cascades of disease. *Nature* **507**, 195–200
7. Donnelly, C. J., Zhang, P. W., Pham, J. T., Haeusler, A. R., Heusler, A. R., Mistry, N. A., Vidensky, S., Daley, E. L., Poth, E. M., Hoover, B., Fines, D. M., Maragakis, N., Tienari, P. J., Petrucelli, L., Traynor, B. J., *et al.* (2013) RNA toxicity from the ALS/FTD C9ORF72 expansion is mitigated by antisense intervention. *Neuron* **80**, 415–428
8. Conlon, E. G., Lu, L., Sharma, A., Yamazaki, T., Tang, T., Shneider, N. A., and Manley, J. L. (2016) The C9ORF72 GGGGCC expansion forms RNA G-quadruplex inclusions and sequesters hnRNP H to disrupt splicing in ALS brains. *Elife* **5**, e17820
9. Fratta, P., Mizielinska, S., Nicoll, A. J., Zloh, M., Fisher, E. M. C., Parkinson, G., and Isaacs, A. M. (2012) C9orf72 hexanucleotide repeat associated with amyotrophic lateral sclerosis and frontotemporal dementia forms RNA G-quadruplexes. *Sci. Rep.* **2**, 1016
10. Su, Z., Zhang, Y., Gendron, T. F., Bauer, P. O., Chew, J., Yang, W.-Y., Fostvedt, E., Jansen-West, K., Belzil, V. V., Desaro, P., Johnston, A., Overstreet, K., Oh, S.-Y., Todd, P. K., Berry, J. D., *et al.* (2014) Discovery of a biomarker and lead small molecules to target r(GGGGCC)-associated defects in c9FTD/ALS. *Neuron* **83**, 1043–1050

11. Zhou, B., Liu, C., Geng, Y., and Zhu, G. (2015) Topology of a G-quadruplex DNA formed by C9orf72 hexanucleotide repeats associated with ALS and FTD. *Sci. Rep.* **5**, 16673
12. Zamiri, B., Reddy, K., Macgregor, R. B., and Pearson, C. E. (2014) TMPyP4 porphyrin distorts RNA G-quadruplex structures of the disease-associated r(GGGGCC)n repeat of the C9orf72 gene and blocks interaction of RNAbinding proteins. *J. Biol. Chem.* **289**, 4653–4659
13. Simone, R., Balendra, R., Moens, T. G., Preza, E., Wilson, K. M., Heslegrave, A., Woodling, N. S., Niccoli, T., Gilbert-Jaramillo, J., Abdelkarim, S., Clayton, E. L., Clarke, M., Konrad, M. T., Nicoll, A. J., Mitchell, J. S., *et al.* (2018) G-quadruplex-binding small molecules ameliorate C9orf72 FTD/ALS pathology in vitro and in vivo. *EMBO Mol. Med.* **10**, 22–31
14. Mendoza, O., Bourdoncle, A., Boulé, J.-B., Brosh, R. M., and Mergny, J.-L. (2016) G-quadruplexes and helicases. *Nucleic Acids Res.* **44**, 1989–2006
15. Maizels, N. (2015) G4-associated human diseases. *EMBO Rep.* **16**, 910–922
16. Rhodes, D., and Lipps, H. J. (2015) G-quadruplexes and their regulatory roles in biology. *Nucleic Acids Res.* **43**, 8627–8637
17. Biffi, G., Tannahill, D., McCafferty, J., and Balasubramanian, S. (2013) Quantitative visualization of DNA G-quadruplex structures in human cells. *Nat. Chem.* **5**, 182–186
18. Henderson, A., Wu, Y., Huang, Y. C., Chavez, E. A., Platt, J., Johnson, F. B., Brosh, R. M., Sen, D., and Lansdorp, P. M. (2014) Detection of G-quadruplex DNA in mammalian cells. *Nucleic Acids Res.* **42**, 860–869
19. Hänsel-Hertsch, R., Beraldi, D., Lensing, S. V., Marsico, G., Zyner, K., Parry, A., Di Antonio, M., Pike, J., Kimura, H., Narita, M., Tannahill, D., and Balasubramanian, S. (2016) G-quadruplex structures mark human regulatory chromatin. *Nat. Genet.* **48**, 1267–1272
20. Chambers, V. S., Marsico, G., Boutell, J. M., Di Antonio, M., Smith, G. P., and Balasubramanian, S. (2015) High-throughput sequencing of DNA G-quadruplex structures in the human genome. *Nat. Biotechnol.* **33**, 877–881
21. Bedrat, A., Lacroix, L., and Mergny, J.-L. (2016) Re-evaluation of G-quadruplex propensity with G4Hunter. *Nucleic Acids Res.* **44**, 1746–1759
22. Huppert, J. L., and Balasubramanian, S. (2005) Prevalence of quadruplexes in the human genome. *Nucleic Acids Res.* **33**, 2908–2916
23. Huppert, J. L., and Balasubramanian, S. (2007) G-quadruplexes in promoters throughout the human genome. *Nucleic Acids Res.* **35**, 406–413
24. Maltby, C. J., Schofield, J. P. R., Houghton, S. D., O'Kelly, I., Vargas-Caballero, M., Deinhardt, K., and Coldwell, M. J. (2020) A 5' UTR GGN repeat controls localisation and translation of a potassium leak channel mRNA through G-quadruplex formation. *Nucleic Acids Res.* **48**, 9822–9839
25. Shi, Y., Lin, S., Staats, K. A., Li, Y., Chang, W. H., Hung, S. T., Hendricks, E., Linares, G. R., Wang, Y., Son, E. Y., Wen, X., Kisler, K., Wilkinson, B., Menendez, L., Sugawara, T., *et al.* (2018) Haploinsufficiency leads to neurodegeneration in C9ORF72 ALS/FTD human induced motor neurons. *Nat. Med.* **24**, 313–325
26. Shi, K. Y., Mori, E., Nizami, Z. F., Lin, Y., Kato, M., Xiang, S., Wu, L. C., Ding, M., Yu, Y., Gall, J. G., and McKnight, S. L. (2017) Toxic PRn poly-dipeptides encoded by the C9orf72 repeat expansion block nuclear import and export. *Proc. Natl. Acad. Sci. U. S. A.* **114**, E1111–E1117
27. Taylor, J. P. (2017) A PR plug for the nuclear pore in amyotrophic lateral sclerosis. *Proc. Natl. Acad. Sci. U. S. A.* **114**, 1445–1447
28. Rodriguez, C. M., and Todd, P. K. (2019) New pathologic mechanisms in nucleotide repeat expansion disorders. *Neurobiol. Dis.* **130**, 104515
29. Green, K. M., Glineburg, M. R., Kearse, M. G., Flores, B. N., Linsalata, A. E., Fedak, S. J., Goldstrohm, A. C., Barmada, S. J., and Todd, P. K. (2017) RAN translation at C9orf72-associated repeat expansions is selectively enhanced by the integrated stress response. *Nat. Commun.* **8**, 2005
30. Cheng, W., Wang, S., Mestre, A. A., Fu, C., Makarem, A., Xian, F., Hayes, L. R., Lopez-Gonzalez, R., Drenner, K., Jiang, J., Cleveland, D. W., and Sun, S. (2018) C9ORF72 GGGGCC repeat-associated non-AUG translation is upregulated by stress through eIF2α phosphorylation. *Nat. Commun.* **9**, 51
31. Tabet, R., Schaeffer, L., Freyermuth, F., Jambeau, M., Workman, M., Lee, C. Z., Lin, C. C., Jiang, J., Jansen-West, K., Abou-Hamdan, H., Désaubry, L., Gendron, T., Petrucelli, L., Martin, F., and Lagier-Tourenne, C. (2018) CUG initiation and frameshifting enable production of dipeptide repeat proteins from ALS/FTD C9ORF72 transcripts. *Nat. Commun.* **9**, 152
32. Sonobe, Y., Ghadge, G., Masaki, K., Sendoel, A., Fuchs, E., and Roos, R. P. (2018) Translation of dipeptide repeat proteins from the C9ORF72 expanded repeat is associated with cellular stress. *Neurobiol. Dis.* **116**, 155–165
33. Linsalata, A. E., He, F., Malik, A. M., Glineburg, M. R., Green, K. M., Natla, S., Flores, B. N., Krans, A., Archbold, H. C., Fedak, S. J., Barmada, S. J., and Todd, P. K. (2019) DDX3X and specific initiation factors modulate FMR1 repeat-associated non-AUG-initiated translation. *EMBO Rep.* **20**, e47498
34. Cheng, W., Wang, S., Zhang, Z., Morgens, D. W., Hayes, L. R., Lee, S., Portz, B., Xie, Y., Nguyen, B. V., Haney, M. S., Yan, S., Dong, D., Coyne, A. N., Yang, J., Xian, F., *et al.* (2019) CRISPR-Cas9 screens identify the RNA helicase DDX3X as a repressor of C9ORF72 (GGGGCC)n repeat-associated non-AUG translation. *Neuron* **104**, 885–898.e8
35. Yamada, S. B., Gendron, T. F., Niccoli, T., Genuth, N. R., Grosely, R., Shi, Y., Glaria, I., Kramer, N. J., Nakayama, L., Fang, S., Dinger, T. J. I., Thoeng, A., Rocha, G., Barna, M., Puglisi, J. D., *et al.* (2019) RPS25 is required for efficient RAN translation of C9orf72 and other neurodegenerative disease-associated nucleotide repeats. *Nat. Neurosci.* **22**, 1383–1388
36. Goodman, L. D., Prudencio, M., Srinivasan, A. R., Rifai, O. M., Lee, V. M.-Y., Petrucelli, L., and Bonini, N. M. (2019) eIF4B and eIF4H mediate GR production from expanded G4C2 in a Drosophila model for C9orf72-associated ALS. *Acta Neuropathol. Commun.* **7**, 62
37. Westergard, T., McAvoy, K., Russell, K., Wen, X., Pang, Y., Morris, B., Pasinelli, P., Trotti, D., and Haeusler, A. (2019) Repeat-associated non-AUG translation in C9orf72-ALS/FTD is driven by neuronal excitation and stress. *EMBO Mol. Med.* **11**, e9423
38. Zu, T., Guo, S., Bardhi, O., Ryskamp, D. A., Li, J., Khoramian Tusi, S., Engelbrecht, A., Klippel, K., Chakrabarty, P., Nguyen, L., Golde, T. E., Sonenberg, N., and Ranum, L. P. W. (2020) Metformin inhibits RAN translation through PKR pathway and mitigates disease in C9orf72 ALS/FTD mice. *Proc. Natl. Acad. Sci. U. S. A.* **117**, 18591–18599
39. Schult, P., and Paeschke, K. (2020) The DEAH helicase DHX36 and its role in G-quadruplex-dependent processes. *Biol. Chem.* **402**, 581–591
40. Creacy, S. D., Routh, E. D., Iwamoto, F., Nagamine, Y., Akman, S. A., and Vaughn, J. P. (2008) G4 resolvase 1 binds both DNA and RNA tetramolecular quadruplex with high affinity and is the major source of tetramolecular quadruplex G4-DNA and G4-RNA resolving activity in HeLa cell lysates. *J. Biol. Chem.* **283**, 34626–34634
41. Vaughn, J. P., Creacy, S. D., Routh, E. D., Joyner-Butt, C., Jenkins, G. S., Pauli, S., Nagamine, Y., and Akman, S. A. (2005) The DEXH protein product of the DHX36 gene is the major source of tetramolecular quadruplex G4-DNA resolving activity in HeLa cell lysates*. *J. Biol. Chem.* **280**, 38117–38120
42. Booy, E. P., McRae, E. K., Howard, R., Deo, S. R., Ariyo, E. O., Dzananovic, E., Meier, M., Stetefeld, J., and McKenna, S. A. (2016) RNA helicase associated with AU-rich element (RHAU/DHX36) interacts with the 3′-tail of the long non-coding RNA BC200 (BCYRN1). *J. Biol. Chem.* **291**, 5355–5372
43. Booy, E. P., Howard, R., Marushchak, O., Ariyo, E. O., Meier, M., Novakowski, S. K., Deo, S. R., Dzananovic, E., Stetefeld, J., and McKenna, S. A. (2014) The RNA helicase RHAU (DHX36) suppresses expression of the transcription factor PITX1. *Nucleic Acids Res.* **42**, 3346–3361
44. Huang, W., Smaldino, P. J., Zhang, Q., Miller, L. D., Cao, P., Stadelman, K., Wan, M., Giri, B., Lei, M., Nagamine, Y., Vaughn, J. P., Akman, S. A., and Sui, G. (2012) Yin Yang 1 contains G-quadruplex structures in its promoter and 5′-UTR and its expression is modulated by G4 resolvase 1. *Nucleic Acids Res.* **40**, 1033–1049
45. Nie, J., Jiang, M., Zhang, X., Tang, H., Jin, H., Huang, X., Yuan, B., Zhang, C., Lai, J. C., Nagamine, Y., Pan, D., Wang, W., and Yang, Z. (2015) Post-transcriptional regulation of Nkx2-5 by RHAU in heart development. *Cell Rep.* **13**, 723–732
46. Kim, H.-N., Lee, J.-H., Bae, S.-C., Ryoo, H.-M., Kim, H.-H., Ha, H., and Lee, Z. H. (2011) Histone deacetylase inhibitor MS-275 stimulates bone

formation in part by enhancing Dhx36-mediated TNAP transcription. *J. Bone Miner. Res.* **26**, 2161–2173
47. Smaldino, P. J., Routh, E. D., Kim, J. H., Giri, B., Creacy, S. D., Hantgan, R. R., Akman, S. A., and Vaughn, J. P. (2015) Mutational dissection of telomeric DNA binding requirements of G4 resolvase 1 shows that G4-structure and certain 3′-tail sequences are sufficient for tight and complete binding. *PLoS One* **10**, e0132668
48. Sexton, A. N., and Collins, K. (2011) The 5′ guanosine tracts of human telomerase RNA are recognized by the G-quadruplex binding domain of the RNA helicase DHX36 and function to increase RNA accumulation. *Mol. Cell. Biol.* **31**, 736–743
49. McRae, E. K. S., Booy, E. P., Moya-Torres, A., Ezzati, P., Stetefeld, J., and McKenna, S. A. (2017) Human DDX21 binds and unwinds RNA guanine quadruplexes. *Nucleic Acids Res.* **45**, 6656–6668
50. Booy, E. P., McRae, E. K. S., and McKenna, S. A. (2015) Biochemical characterization of G4 quadruplex telomerase RNA unwinding by the RNA helicase RHAU. *Methods Mol. Biol.* **1259**, 125–135
51. Booy, E. P., Meier, M., Okun, N., Novakowski, S. K., Xiong, S., Stetefeld, J., and McKenna, S. A. (2012) The RNA helicase RHAU (DHX36) unwinds a G4-quadruplex in human telomerase RNA and promotes the formation of the P1 helix template boundary. *Nucleic Acids Res.* **40**, 4110–4124
52. Giri, B., Smaldino, P. J., Thys, R. G., Creacy, S. D., Routh, E. D., Hantgan, R. R., Lattmann, S., Nagamine, Y., Akman, S. A., and Vaughn, J. P. (2011) G4 resolvase 1 tightly binds and unwinds unimolecular G4-DNA. *Nucleic Acids Res.* **39**, 7161–7178
53. Sauer, M., Juranek, S. A., Marks, J., De Magis, A., Kazemier, H. G., Hilbig, D., Benhalevy, D., Wang, X., Hafner, M., and Paeschke, K. (2019) DHX36 prevents the accumulation of translationally inactive mRNAs with G4-structures in untranslated regions. *Nat. Commun.* **10**, 2421
54. Vester, K., Eravci, M., Serikawa, T., Schütze, T., Weise, C., and Kurreck, J. (2019) RNAi-mediated knockdown of the Rhau helicase preferentially depletes proteins with a Guanine-quadruplex motif in the 5′-UTR of their mRNA. *Biochem. Biophys. Res. Commun.* **508**, 756–761
55. Murat, P., Marsico, G., Herdy, B., Ghanbarian, A., Portella, G., and Balasubramanian, S. (2018) RNA G-quadruplexes at upstream open reading frames cause DHX36- and DHX9-dependent translation of human mRNAs. *Genome Biol.* **19**, 229
56. Chen, M. C., Tippana, R., Demeshkina, N. A., Murat, P., Balasubramanian, S., Myong, S., and Ferré-D'Amaré, A. R. (2018) Structural basis of G-quadruplex unfolding by the DEAH/RHA helicase DHX36. *Nature* **558**, 465–469
57. Iwamoto, F., Stadler, M., Chalupníková, K., Oakeley, E., and Nagamine, Y. (2008) Transcription-dependent nucleolar cap localization and possible nuclear function of DExH RNA helicase RHAU. *Exp. Cell Res.* **314**, 1378–1391
58. Schmidt, E. K., Clavarino, G., Ceppi, M., and Pierre, P. (2009) SUnSET, a nonradioactive method to monitor protein synthesis. *Nat. Methods* **6**, 275–277
59. Todd, P. K., Oh, S. Y., Krans, A., He, F., Sellier, C., Frazer, M., Renoux, A. J., Chen, K.-C., Scaglione, K. M., Basrur, V., Elenitoba-Johnson, K., Vonsattel, J. P., Louis, E. D., Sutton, M. A., Taylor, J. P., *et al.* (2013) CGG repeat-associated translation mediates neurodegeneration in fragile X tremor ataxia syndrome. *Neuron* **78**, 440–455
60. Krans, A., Kearse, M. G., and Todd, P. K. (2016) Repeat-associated non-AUG translation from antisense CCG repeats in fragile X tremor/ataxia syndrome. *Ann. Neurol.* **80**, 871–881
61. Buijsen, R. A., Visser, J. A., Kramer, P., Severijnen, E. A., Gearing, M., Charlet-Berguerand, N., Sherman, S. L., Berman, R. F., Willemsen, R., and Hukema, R. K. (2016) Presence of inclusions positive for polyglycine containing protein, FMRpolyG, indicates that repeat-associated non-AUG translation plays a role in fragile X-associated primary ovarian insufficiency. *Hum. Reprod.* **31**, 158–168
62. Sellier, C., Buijsen, R. A. M., He, F., Natla, S., Jung, L., Tropel, P., Gaucherot, A., Jacobs, H., Meziane, H., Vincent, A., Champy, M.-F., Sorg, T., Pavlovic, G., Wattenhofer-Donze, M., Birling, M.-C., *et al.* (2017) Translation of expanded CGG repeats into FMRpolyG is pathogenic and may contribute to fragile X tremor ataxia syndrome. *Neuron* **93**, 331–347
63. Buijsen, R. A., Sellier, C., Severijnen, L.-A. W., Oulad-Abdelghani, M., Verhagen, R. F., Berman, R. F., Charlet-Berguerand, N., Willemsen, R., and Hukema, R. K. (2014) FMRpolyG-positive inclusions in CNS and non-CNS organs of a fragile X premutation carrier with fragile X-associated tremor/ataxia syndrome. *Acta Neuropathol. Commun.* **2**, 162
64. Hukema, R. K., Buijsen, R. A., Schonewille, M., Raske, C., Severijnen, L. A., Nieuwenhuizen-Bakker, I., Verhagen, R. F., van Dessel, L., Maas, A., Charlet-Berguerand, N., De Zeeuw, C. I., Hagerman, P. J., Berman, R. F., and Willemsen, R. (2015) Reversibility of neuropathology and motor deficits in an inducible mouse model for FXTAS. *Hum. Mol. Genet.* **24**, 4948–4957
65. Usdin, K., and Woodford, K. J. (1995) CGG repeats associated with DNA instability and chromosome fragility form structures that block DNA synthesis *in vitro*. *Nucleic Acids Res.* **23**, 4202–4209
66. Fry, M., and Loeb, L. A. (1994) The fragile X syndrome d(CGG)(n) nucleotide repeats form a stable tetrahelical structure. *Proc. Natl. Acad. Sci. U. S. A.* **91**, 4950–4954
67. Kettani, A., Kumar, A. R., and Patel, D. J. (1995) Solution structure of a DNA quadruplex containing the fragile X syndrome triplet repeat. *J. Mol. Biol.* **254**, 638–656
68. Asamitsu, S., Yabuki, Y., Ikenoshita, S., Kawakubo, K., Kawasaki, M., Usuki, S., Nakayama, Y., Adachi, K., Kugoh, H., Ishii, K., Matsuura, T., Nanba, E., Sugiyama, H., Fukunaga, K., and Shioda, N. (2021) CGG repeat RNA G-quadruplexes interact with FMRpolyG to cause neuronal dysfunction in fragile X-related tremor/ataxia syndrome. *Sci. Adv.* **7**, eabd9440
69. Kearse, M. G., Green, K. M., Krans, A., Rodriguez, C. M., Linsalata, A. E., Goldstrohm, A. C., and Todd, P. K. (2016) CGG repeat-associated non-AUG translation utilizes a cap-dependent scanning mechanism of initiation to produce toxic proteins. *Mol. Cell* **62**, 314–322
70. Almeida, S., Krishnan, G., Rushe, M., Gu, Y., Kankel, M. W., and Gao, F.-B. (2019) Production of poly(GA) in C9ORF72 patient motor neurons derived from induced pluripotent stem cells. *Acta Neuropathol.* **138**, 1099–1101
71. Jackson, R. J., Hellen, C. U., and Pestova, T. V. (2010) The mechanism of eukaryotic translation initiation and principles of its regulation. *Nat. Rev. Mol. Cell Biol.* **11**, 113–127
72. Walter, P., and Ron, D. (2011) The unfolded protein response: From stress pathway to homeostatic regulation. *Science* **334**, 1081–1086
73. Young, S. K., Baird, T. D., and Wek, R. C. (2016) Translation regulation of the glutamyl-prolyl-tRNA synthetase gene EPRS through bypass of upstream open reading frames with noncanonical initiation codons. *J. Biol. Chem.* **291**, 10824–10835
74. Starck, S. R., Tsai, J. C., Chen, K., Shodiya, M., Wang, L., Yahiro, K., Martins-Green, M., Shastri, N., and Walter, P. (2016) Translation from the 5′ untranslated region shapes the integrated stress response. *Science* **351**, aad3867
75. Hinnebusch, A. G., Ivanov, I. P., and Sonenberg, N. (2016) Translational control by 5′-untranslated regions of eukaryotic mRNAs. *Science* **352**, 1413–1416
76. Simone, R., Fratta, P., Neidle, S., Parkinson, G. N., and Isaacs, A. M. (2015) G-quadruplexes: Emerging roles in neurodegenerative diseases and the non-coding transcriptome. *FEBS Lett.* **589**, 1653–1668
77. Schofield, J. P. R., Cowan, J. L., and Coldwell, M. J. (2015) G-quadruplexes mediate local translation in neurons. *Biochem. Soc. Trans.* **43**, 338–342
78. Brunelle, J. L., and Green, R. (2013) *In vitro* transcription from plasmid or PCR-amplified DNA. *Methods Enzymol.* **530**, 101–114
79. Zu, T., Liu, Y., Bañez-Coronel, M., Reid, T., Pletnikova, O., Lewis, J., Miller, T. M., Harms, M. B., Falchook, A. E., Subramony, S. H., Ostrow, L. W., Rothstein, J. D., Troncoso, J. C., and Ranum, L. P. (2013) RAN proteins and RNA foci from antisense transcripts in C9ORF72 ALS and frontotemporal dementia. *Proc. Natl. Acad. Sci. U. S. A.* **110**, E4968–E4977
80. Liu, H., Lu, Y. N., Paul, T., Periz, G., Banco, M. T., Ferré-D'Amaré, A. R., Rothstein, J. D., Hayes, L. R., Myong, S., and Wang, J. (2021) A helicase unwinds hexanucleotide repeat RNA G-quadruplexes and facilitates repeat-associated non-AUG translation. *J. Am. Chem. Soc.* **143**, 7368–7379

81. Westergard, T., Jensen, B. K., Wen, X., Cai, J., Kropf, E., Iacovitti, L., Pasinelli, P., and Trotti, D. (2016) Cell-to-cell transmission of dipeptide repeat proteins linked to C9orf72-ALS/FTD. *Cell Rep.* **17**, 645–652
82. Chalupníková, K., Lattmann, S., Selak, N., Iwamoto, F., Fujiki, Y., and Nagamine, Y. (2008) Recruitment of the RNA helicase RHAU to stress granules via a unique RNA-binding domain. *J. Biol. Chem.* **283**, 35186–35198
83. Byrd, A. K., Zybailov, B. L., Maddukuri, L., Gao, J., Marecki, J. C., Jaiswal, M., Bell, M. R., Griffin, W. C., Reed, M. R., Chib, S., Mackintosh, S. G., MacNicol, A. M., Baldini, G., Eoff, R. L., and Raney, K. D. (2016) Evidence that G-quadruplex DNA accumulates in the cytoplasm and participates in stress granule assembly in response to oxidative stress. *J. Biol. Chem.* **291**, 18041–18057
84. Yoo, J.-S., Takahasi, K., Ng, C. S., Ouda, R., Onomoto, K., Yoneyama, M., Lai, J. C., Lattmann, S., Nagamine, Y., Matsui, T., Iwabuchi, K., Kato, H., and Fujita, T. (2014) DHX36 enhances RIG-I signaling by facilitating PKR-mediated antiviral stress granule formation. *PLoS Pathog.* **10**, e1004012
85. Stoneley, M., and Willis, A. E. (2004) Cellular internal ribosome entry segments: Structures, trans-acting factors and regulation of gene expression. *Oncogene* **23**, 3200–3207
86. Komar, A. A., and Hatzoglou, M. (2011) Cellular IRES-mediated translation: The war of ITAFs in pathophysiological states. *Cell Cycle* **10**, 229–240
87. Komar, A. A., and Hatzoglou, M. (2005) Internal ribosome entry sites in cellular mRNAs: Mystery of their existence. *J. Biol. Chem.* **280**, 23425–23428